SCIENCE CHINA
Information Sciences

• RESEARCH PAPER •

June 2012 Vol. 55 No. 6: 1270–1279
doi: 10.1007/s11432-011-4320-x

A novel fractional wavelet transform and its applications

SHI Jun*, ZHANG NaiTong & LIU XiaoPing

Communication Research Center, Harbin Institute of Technology, Harbin 150001*, China*

Received March 30, 2010; accepted March 29, 2011; published online September 9, 2011

Abstract The wavelet transform (WT) and the fractional Fourier transform (FRFT) are powerful tools for many applications in the field of signal processing. However, the signal analysis capability of the former is limited in the time-frequency plane. Although the latter has overcome such limitation and can provide signal representations in the fractional domain, it fails in obtaining local structures of the signal. In this paper, a novel fractional wavelet transform (FRWT) is proposed in order to rectify the limitations of the WT and the FRFT. The proposed transform not only inherits the advantages of multiresolution analysis of the WT, but also has the capability of signal representations in the fractional domain which is similar to the FRFT. Compared with the existing FRWT, the novel FRWT can offer signal representations in the time-fractional-frequency plane. Besides, it has explicit physical interpretation, low computational complexity and usefulness for practical applications. The validity of the theoretical derivations is demonstrated via simulations.

Keywords time-frequency analysis, wavelet transform, multiresolution analysis, fractional Fourier transform, time-fractional-frquency analysis

Citation Shi J, Zhang N T, Liu X P. A novel fractional wavelet transform and its applications. Sci China Inf Sci, 2011, 54: 1270–1279, doi: 10.1007/s11432-011-4320-x

1 Introduction

The wavelet transform (WT) has been shown to be an appropriate tool for time-frequency analysis. It has been applied in many fields of signal processing, including speech, image, communications, radar [1], etc. However, under the extension of research objects and scope, the WT has been discovered to have shortcomings. Since each wavelet component is actually a differently scaled bandpass filter in the frequency domain, the signal analysis capability of the WT is limited in the time-frequency plane and, therefore, the WT is inefficient for processing signals whose energy is not well concentrated in the frequency domain. For example, chirp-like signals [2], which are ubiquitous in nature and man-made systems, are this kind of signals [3]. So a series of novel signal processing tools have been proposed to analyze such signals, such as: the fractional wavelet transform (FRWT) [4–7], the fractional Fourier transform (FRFT) [8], the short-time FRFT [9], the Radon-Wigner transform [10] and so on. However, the Radon-Wigner transform has cross-term problem because it is the quadratic time-frequency representation. Although the FRFT has a number of unique properties, it cannot obtain information about local properties of the signal. In addition, the drawback of the short-time FRFT is that its time- and fractional-domain resolutions can not

*Corresponding author (email: j.shi@yahoo.cn)

simultaneously be arbitrarily high. As a generalization of the WT, the FRWT combines the advantages of the WT and the FRFT, i.e., it is a linear transformation without cross-term interference and is capable of providing multiresolution analysis and representing signals in the fractional domain. Thus, the FRWT may be potentially useful in the signal processing community and will attract more and more attention.

In 1997, Mendlovic et al. [4] first introduced the FRWT as a way to deal with optical signals. The idea behind this transform is deriving the fractional spectrum of the signal by using the FRFT and performing the WT of the fractional spectrum. Since the FRFT tells us the fractional frequencies that lasts for the total duration of the signal rather than for a particular time, the fractional spectrum of the signal cannot be ascertained when those fractional frequencies exist. Therefore, the FRWT [4] fails in obtaining information about local properties of the signal and, thus, it has been applied only for image entropy [5, 6] so far. Shortly after, in 1998, Huang and Suter [7] proposed the concept of the fractional wave packet transform (FRWPT). Unfortunately, the FRWPT did not receive much attention for the lack of physical interpretation and high computational complexity. In some works, the WT based on the fractional B-splines is also called as the FRWT [11]. Since this transform is actually a scaled bandpass filter in the frequency domain and cannot represent signals in the fractional domain, it still belongs to the traditional WT. The aim of this paper is to introduce a novel fractional wavelet transform (NFRWT) to circumvent the limitations of the WT and the FRFT. The proposed transform has explicit physical interpretation, i.e., each fractional wavelet component is actually a differently scaled bandpass filter in the fractional domain, and it has much lower computational complexity than those introduced in [4, 7].

The rest of the paper is organized as follows. In the next section, definitions of the WT and the FRFT are briefly introduced and the fractional convolution theorem of the FRFT is given. In Section 3, the novel fractional wavelet transform (NFRWT) is proposed. Moreover, basic properties, the inverse formula, and the admissibility condition of the NFRWT are also derived. In Section 4, the time-fractional-frequency analysis of the NFRWT is discussed. Some applications of the NFRWT are examined and simulations are given in Section 5. Conclusions appear at the end of the paper.

2 Preliminaries

2.1 Wavelet transform

The classical convolution of two time domain functions $f(t)$ and $g(t)$ is defined as

$$f(t) * g(t) = \int_{-\infty}^{+\infty} f(\tau) g(t-\tau)\,\mathrm{d}\tau = \langle f(\cdot), g^*(t-\cdot)\rangle\,, \tag{1}$$

where $*$ and * in the subscript denote the classical convolution operator and the complex conjugate, respectively, and $\langle\cdot,\cdot\rangle$ indicates the inner product. Furthermore, the classical convolution theorem of the Fourier transform (FT) is given by

$$f(t) * g(t) \xleftrightarrow{\mathfrak{F}} \sqrt{2\pi} F(\omega) G(\omega), \tag{2}$$

where $\mathfrak{F}$ denotes the FT operator. $F(\omega)$ and $G(\omega)$ stands for the FT of $f(t)$ and $g(t)$, respectively.

The wavelet transform (WT) [1] of a signal $x(t) \in L^2(\mathbb{R})$ can be defined as a classical convolution, i.e.,

$$W_x(a,b) = x(t) * \left(a^{-\frac{1}{2}} \psi^*\left(-t/a\right)\right) = \langle x(\cdot), \psi_{a,b}(\cdot)\rangle\,, \tag{3}$$

where the kernel $\psi_{a,b}(t)$ is a continuous affine transformation of the mother wavelet $\psi(t)$, i.e.,

$$\psi_{a,b}(t) = \frac{1}{\sqrt{a}} \psi\left(\frac{t-b}{a}\right), \tag{4}$$

where $a \in \mathbb{R}^+$ and $b \in \mathbb{R}$ are respectively scaling and translation parameters. It follows from the classical convolution theorem and the inverse FT that the WT of the signal $x(t)$ can be also expressed as

$$W_x(a,b) = \int_{-\infty}^{+\infty} \sqrt{2\pi a} X(\omega) \Psi^*(a\omega) \mathrm{e}^{\mathrm{j}\omega b}\,\mathrm{d}\omega, \tag{5}$$

where $X(\omega)$ and $\Psi(\omega)$ denote the FT of $x(t)$ and $\psi(t)$, respectively. Since $\Psi(0) = \int_{-\infty}^{+\infty} \psi(t)\mathrm{d}t = 0$, the WT is actually a bandpass filter in the frequency domian. Thus, signal analysis associated with it is limited to the time-frequency plane. As for signals whose energy is not well concentrated in the frequency domain, results obtained using the WT will be not optimal.

2.2 Fractional Fourier transform and fractional convolution theorem

The fractional Fourier transform (FRFT) of a signal $x(t) \in L^2(\mathbb{R})$ is defined as [8]

$$X_\alpha(u) = \mathcal{F}^\alpha[x](u) = \int_{-\infty}^{+\infty} x(t)\mathcal{K}_\alpha(u,t)\,\mathrm{d}t \tag{6}$$

where $\mathcal{F}^\alpha$ denotes the FRFT operator and the kernel $\mathcal{K}_\alpha(u,t)$ is given by

$$\mathcal{K}_\alpha(u,t) = \begin{cases} \sqrt{\frac{1-\mathrm{j}\cot\theta}{2\pi}}\mathrm{e}^{(\mathrm{j}/2)(u^2+t^2)\cot\theta - \mathrm{j}ut\csc\theta}, & \alpha \neq k, \\ \delta(t-u), & \alpha = 2k, \\ \delta(t+u), & \alpha = 2k+1, \end{cases} \tag{7}$$

where α denotes the order of the FRFT, $\theta{=}\alpha\pi/2$ is the rotation angle. The u axis is regarded as the fractional domain, and the variable u is the fractional frequency. The inverse FRFT is the FRFT with order $-\alpha$. Whenever $\alpha{=}1$, the FRFT reduces to the FT.

The FRFT is different from the FT because of the unique properties, and it has been widely applied in signal processing community in recent years [3,8,12–16]. However, the FRFT tells us the fractional frequencies that exist across the whole duration of the signal but not the fractional frequencies which exist only at a particular time. This means that the FRFT is a global transformation so that it fails in obtaining any local information of the signal, which are essential and pivotal for processing non-stationary signals [10].

The fractional convolution of the FRFT for functions $x(t)$ and $h(t)$ can be defined as [12]

$$x(t)\Theta_\alpha h(t) = \mathrm{e}^{-(\mathrm{j}/2)t^2\cot\theta} \cdot \left[\left(x(t)\mathrm{e}^{(\mathrm{j}/2)t^2\cot\theta}\right) * h(t)\right] = \mathrm{e}^{-(\mathrm{j}/2)t^2\cot\theta} \cdot \left\langle x(\cdot)\mathrm{e}^{(\mathrm{j}/2)(\cdot)^2\cot\theta}, h^*(t-\cdot)\right\rangle, \tag{8}$$

where Θ_α denotes the fractional convolution operator. Let $X_\alpha(u)$ indicate the FRFT of $x(t)$, and $H(u\csc\theta)$ be the FT (with its argument scaled by $\csc\theta$) of $h(t)$. Then, the fractional convolution theorem of the FRFT is given by

$$x(t)\Theta_\alpha h(t) \overset{\mathcal{F}^\alpha}{\longleftrightarrow} \sqrt{2\pi}X_\alpha(u)H(u\csc\theta), \tag{9}$$

which demonstrates that a time-domain fractional convolution is equivalent to a simple fractional-domain multiplication. Particularly, when $\alpha{=}1$, (8) reduces to the classical convolution as given by (1).

3 Novel fractional wavelet transform

3.1 Definition of novel fractional wavelet transform

Motivated by the relationship between the WT and the classical convolution in (3), one would naturally expect that there exists a similar relationship between the FRWT and the fractional convolution. Thus, we define a novel fractional wavelet transform (NFRWT) with an order α of a square integrable signal $x(t)$ as

$$\begin{aligned} W_x^\alpha(a,b) &= x(t)\Theta_\alpha\left(a^{-\frac{1}{2}}\psi^*\left(-t/a\right)\right) = \mathrm{e}^{-(\mathrm{j}/2)b^2\cot\theta} \cdot \left\langle x(\cdot)\mathrm{e}^{(\mathrm{j}/2)(\cdot)^2\cot\theta}, \psi_{a,b}(\cdot)\right\rangle \\ &= \int_{-\infty}^{+\infty} x(t)\psi^*_{\alpha,a,b}(t)\mathrm{d}t, \end{aligned} \tag{10}$$

where the kernel $\psi_{\alpha,a,b}(t)$ satisfies

$$\psi_{\alpha,a,b}(t) = \mathrm{e}^{-(\mathrm{j}/2)(t^2-b^2)\cot\theta}\psi_{a,b}(t), \tag{11}$$

where $\psi_{a,b}(t)$ is expressed in (4). Note that when α=1, the NFRWT coincides with the WT.

It follows from (9) and the inverse FRFT that the NFRWT can be expressed in terms of the FRFT $X_\alpha(u)$ of the signal $x(t)$

$$W_x^\alpha(a,b) = \int_{-\infty}^{+\infty} \sqrt{2\pi a} X_\alpha(u)\Psi^*(au\csc\theta)\mathcal{K}_{-\alpha}(u,b)\,\mathrm{d}u, \tag{12}$$

where $\Psi(u\csc\theta)$ denotes the FT (with its argument scaled by $\csc\theta$) of $\psi(t)$. (12) states that each fractional wavelet component is actually a differently scaled bandpass filter in the fractional domain. This means that the NFRWT can overcome the weakness of the WT whose analysis is limited to the time-frequency plane and circumvent the above mentioned drawback of the FRFT, as will be elaborated in detail in section 4.

Further, the definition of the NFRWT in (10) can be rewritten as

$$W_x^\alpha(a,b) = \mathrm{e}^{-(\mathrm{j}/2)b^2\cot\theta}\int_{-\infty}^{+\infty}\left(x(t)\mathrm{e}^{(\mathrm{j}/2)t^2\cot\theta}\right)\psi_{a,b}^*(t)\,\mathrm{d}t. \tag{13}$$

Evidently, the computation of the NFRWT corresponds to the following steps:

1) a product by a chirp signal, i.e., $x(t) \to \hat{x}(t)$=$x(t)\mathrm{e}^{(\mathrm{j}/2)t^2\cot\theta}$.

2) a traditional WT, i.e., $\hat{x}(t) \to W_{\hat{x}}(a,b)$.

3) another product by a chirp signal, i.e., $W_{\hat{x}}(a,b) \to W_x^\alpha(a,b)$=$W_{\hat{x}}(a,b)\mathrm{e}^{-(\mathrm{j}/2)b^2\cot\theta}$.

Since the input signal (e.g., a digital signal) is processed by a digital computing machine, it is prudent to define the discrete version of each step. First, multiply the function $x(t)$ with a chirp signal $\mathrm{e}^{(\mathrm{j}/2)t^2\cot\theta}$, and sample the multiplied signal $\hat{x}(t)$. Next, discretize the scaling and translation parameters a and b. The most popular approach of discretizing a and b is using $a = 2^m$, $b = n2^m$ where m and n are integers. Then, perform a discrete WT on the samples of $\hat{x}(t)$. Finally, after multiplying another chirp signal $\mathrm{e}^{-(\mathrm{j}/2)b^2\cot\theta}$, the NFRWT of the signal $x(t)$ is obtained. It follows that the computational complexity of the NFRWT depends on that of the WT which has $O(N)$(N is the length of the sequence) implementation time. So, the computational complexity of the NFRWT is $O(N)$. In contrast, the complexity of computation for the FRWT introduced in [4] and [7] is $O(N^3\log_2 N)$ and $O(N+N\log_2 N)$, respectively. Thus, the NFRWT is easy to implement for practical applications. Figure 1 shows the comparison of the computational complexity of the NFRWT and the FRWT introduced in [4,7]. Moreover, the computation of the FRWT [4,7] needs the discrete algorithm of the FRFT, and there still exists no satisfactory discrete algorithm for the FRFT so far [13]. The NFRWT can be implemented by the discrete algorithm of the WT and does not need the discrete algorithm of the FRFT.

3.2 Basic properties of novel fractional wavelet transfrom

3.2.1 *Linearity property*

If $x(t) = k_1x_1(t) + k_2x_2(t)$, and $x_1(t) \leftrightarrow W_{x_1}^\alpha(a,b)$, $x_2(t) \leftrightarrow W_{x_2}^\alpha(a,b)$, then it is easy to verify that

$$W_x^\alpha(a,b) = k_1W_{x_1}^\alpha(a,b) + k_2W_{x_2}^\alpha(a,b). \tag{14}$$

3.2.2 *Scaling property*

If $x(t) \leftrightarrow W_x^\alpha(a,b)$, then

$$\begin{aligned}\int_{-\infty}^{+\infty} x(ct)\psi_{\alpha,a,b}^*(t)\mathrm{d}t &= \int_{-\infty}^{+\infty} x(ct)\mathrm{e}^{(\mathrm{j}/2)(t^2-b^2)\cot\theta}\frac{1}{\sqrt{a}}\psi^*\left(\frac{t-b}{a}\right)\mathrm{d}t\\ &= \frac{1}{\sqrt{c}}\int_{-\infty}^{+\infty} x(t')\mathrm{e}^{(\mathrm{j}/2)(t'^2-(bc)^2)\cot\varphi}\frac{1}{\sqrt{ac}}\psi^*\left(\frac{t'-bc}{ac}\right)\mathrm{d}t' = \frac{1}{\sqrt{c}}W_x^\beta(ac,bc),\end{aligned} \tag{15}$$

where $c \in \mathbb{R}^+$, $\varphi = \mathrm{arccot}(c^2\cot\theta)$, and $\beta = \varphi/(\pi/2)$.

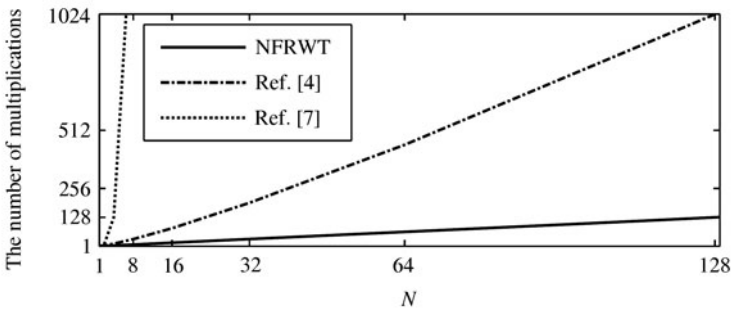

Figure 1 Comparison of the computation complexity of the NFRWT and the existing FRWT.

3.2.3 *Inner product theorem*

Theorem 1. Let $W_x^\alpha(a,b)$ and $W_g^\alpha(a,b)$ denote the αth NFRWT of $x(t), g(t) \in L^2(\mathbb{R})$, and let $\Psi(\Omega)$ denote the FT of $\psi(t)$. If $\Psi(\Omega)$ satisfies

$$C_\psi = \int_{-\infty}^{+\infty} \frac{|\Psi(\Omega)|^2}{\Omega}\,\mathrm{d}\Omega < \infty. \tag{16}$$

Then,

$$\iint_{-\infty}^{+\infty} W_x^\alpha(a,b)\left[W_g^\alpha(a,b)\right]^* \frac{\mathrm{d}a}{a^2}\,\mathrm{d}b = 2\pi C_\psi \left\langle x(\cdot), g(\cdot)\right\rangle. \tag{17}$$

Proof. It follows from (12) that

$$W_x^\alpha(a,b) = \int_{-\infty}^{+\infty} \sqrt{2\pi a} X_\alpha(u)\Psi^*(au\csc\theta)\mathcal{K}_{-\alpha}(u,b)\,\mathrm{d}u, \tag{18}$$

$$W_g^\alpha(a,b) = \int_{-\infty}^{+\infty} \sqrt{2\pi a} G_\alpha(u')\Psi^*(au'\csc\theta)\mathcal{K}_{-\alpha}(u',b)\,\mathrm{d}u'. \tag{19}$$

Next, inserting (18) and (19) into (17) results in

$$\iint_{-\infty}^{+\infty} W_x^\alpha(a,b)\left[W_g^\alpha(a,b)\right]^* \frac{\mathrm{d}a}{a^2}\mathrm{d}b = 2\pi \int_{-\infty}^{+\infty} \frac{|\Psi(au\csc\theta)|^2}{a}\mathrm{d}a \int_{-\infty}^{+\infty} X_\alpha(u)G_\alpha^*(u)\,\mathrm{d}u. \tag{20}$$

Then, by utilizing the inner product theorem of the FRFT [8] and (20), (17) can be established. This completes the proof of the Theorem 1.

3.2.4 *Parseval's relation*

Theorem 2. For any function $x(t) \in L^2(\mathbb{R})$, let $W_x^\alpha(a,b)$ denote the NFRWT of $x(t)$. Then,

$$\int_{-\infty}^{+\infty} |x(t)|^2\,\mathrm{d}t = \frac{1}{2\pi C_\psi} \iint_{-\infty}^{+\infty} |W_x^\alpha(a,b)|^2 \frac{\mathrm{d}a}{a^2}\mathrm{d}b, \tag{21}$$

where one can define an energy density called a fractional scalogram, denoted by $|W_x^\alpha(a,b)|^2$. The proof of Theorem 2 can be easily deduced by setting $g(t) = x(t)$ in Theorem 1 and is omitted.

Theorem 2 states that the αth fractional scalogram shows how the energy of the signal is distributed in the αth time-scale plane. This is a generalization of the fact that the scalogram of the WT measures the energy of the signal in the ordinary time-scale plane.

3.3 Inversion formula and admissibility condition

Theorem 3. Let $\Psi(\Omega)$ denote the FT of $\psi(t)$. If $x(t)$, $\psi(t) \in L^2(\mathbb{R})$, and $\Psi(\Omega)$ satisfies (16), then the inversion formula of the NFRWT is given by

$$x(t) = \frac{1}{2\pi C_\psi} \iint_{-\infty}^{+\infty} W_x^\alpha(a,b)\psi_{\alpha,a,b}(t)\frac{\mathrm{d}a}{a^2}\mathrm{d}b. \tag{22}$$

The proof of Theorem 3 can be easily derived by setting $g(t) = \delta(t)$ in Theorem 1 and is omitted here. Both Theorem 3 and Theorem 2 hold for $C_\psi < \infty$ which is called the admissibility condition for the NFRWT. It follows from the condition that $\Psi(0) = 0$, and therefore, the NFRWT is intrinsically a bank of multiscale bandpass filters in the fractional domain.

4 Time-fractional-frequency analysis

4.1 Constant-Q property

According to (10) and (12), if the kernel of the NFRWT $\psi_{\alpha,a,b}(t)$ is supported in the time domain, then the inner product of $x(t)$ and $\psi_{\alpha,a,b}(t)$ can ensure that $W_x^\alpha(a,b)$ is supported in the time domain too. Therefore, $W_x^\alpha(a,b)$ contains information about $x(t)$ near b. Similarly, if $\Psi^*(u\csc\theta)$ is bandpass, i.e., $\Psi(\Omega)$ satisfies the admissibility condition in (16), then, the multiplication of $X_\alpha(u)$ and $\Psi^*(au\csc\theta)$ can provide fractional-domain local properties of $x(t)$. This implies that the NFRWT is capable of providing the time- and fractional-domain information simultaneously, hence giving a time-fractional-frequency representation of the signal. To be specific, both $\psi(t)$ and its FT $\Psi(\omega)$ must have sufficiently fast decay so that they can be used as window functions. Suppose that $\psi(t)$ and $\Psi(\omega)$ are functions with finite centers E_ψ and E_Ψ and finite radii Δ_ψ and Δ_Ψ. Then, the center and radii of the time-domain window function $\psi_{\alpha,a,b}(t)$ of the NFRWT are respectively given by

$$E[\psi_{\alpha,a,b}(t)] = \frac{\int_{-\infty}^{+\infty} t|\psi_{\alpha,a,b}(t)|^2\mathrm{d}t}{\int_{-\infty}^{+\infty}|\psi_{\alpha,a,b}(t)|^2\mathrm{d}t} = \frac{\int_{-\infty}^{+\infty} t|\psi_{a,b}(t)|^2\mathrm{d}t}{\int_{-\infty}^{+\infty}|\psi_{a,b}(t)|^2\mathrm{d}t} = E\left[\psi_{a,b}(t)\right] = b + aE_\psi, \tag{23}$$

$$\begin{aligned}\Delta[\psi_{\alpha,a,b}(t)] &= \left(\frac{\int_{-\infty}^{+\infty}(t-b-aE_\psi)^2|\psi_{\alpha,a,b}(t)|^2\mathrm{d}t}{\int_{-\infty}^{+\infty}|\psi_{\alpha,a,b}(t)|^2\mathrm{d}t}\right)^{\frac{1}{2}}\\ &= \left(\frac{\int_{-\infty}^{+\infty}(t-b-aE_\psi)^2|\psi_{a,b}(t)|^2\mathrm{d}t}{\int_{-\infty}^{+\infty}|\psi_{a,b}(t)|^2\mathrm{d}t}\right)^{\frac{1}{2}}\\ &= \Delta[\psi_{a,b}(t)] = a\Delta_\psi,\end{aligned} \tag{24}$$

where $E[\cdot]$ and $\Delta[\cdot]$ denote the expectation and deviation operator, respectively. Similarly, the center and radii of the frequency-domain window function $\Psi(a\omega)$ of the WT can be easily derived as

$$E[\Psi(a\omega)] = \frac{E_\Psi}{a}, \quad \Delta[\Psi(a\omega)] = \frac{\Delta_\Psi}{a}. \tag{25}$$

Next, substituting $\omega = u\csc\theta$ into (25) and applying (12) result in

$$E[\Psi(au\csc\theta)] = \frac{E_\Psi}{a}\sin\theta, \quad \Delta[\Psi(au\csc\theta)] = \frac{\Delta_\Psi}{a}\sin\theta, \tag{26}$$

which indicate the center and radii of the fractional-domain window function $\Psi(au\csc\theta)$ of the NFRWT, respectively. Then, the Q-factor (or the ratio between the width and the center) of the fractional-domain window function of the NFRWT is given by

$$Q = \frac{\Delta[\Psi(au\csc\theta)]}{E[\Psi(au\csc\theta)]} = \frac{(\Delta_\Psi/a)\sin\theta}{(E_\Psi/a)\sin\theta} = \frac{\Delta_\Psi}{E_\Psi}, \tag{27}$$

which is independent of the order α ($\theta = \alpha\pi/2$) and the scaling parameter a. This is the constant-Q property of the NFRWT.

4.2 Time-fractional-frequency resolution

From (23), (24) and (10), it follows that the NFRWT $W_x^\alpha(a,b)$ of a signal $x(t)$ localizes the signal with a time window

$$[b + aE_\psi - a\Delta_\psi, b + aE_\psi + a\Delta_\psi]. \tag{28}$$

This is called time localization in signal analysis. Moreover, according to (12) and (26), the same quantity $W_x^\alpha(a,b)$ also gives localized information of the fractional spectrum $X_\alpha(u)$ of the signal $x(t)$, with a fractional frequency window

$$\left[\frac{E_\Psi}{a} - \frac{\Delta_\Psi}{a}, \frac{E_\Psi}{a} + \frac{\Delta_\Psi}{a}\right] \cdot \sin\theta. \tag{29}$$

This is called fractional frequency localization. By equating the quantities $W_x^\alpha(a,b)$ in (10) and (12), we now have a time-fractional-frequency window

$$[b + aE_\psi - a\Delta_\psi, b + aE_\psi + a\Delta_\psi] \times \left[\frac{E_\Psi}{a} - \frac{\Delta_\Psi}{a}, \frac{E_\Psi}{a} + \frac{\Delta_\Psi}{a}\right] \cdot \sin\theta, \tag{30}$$

with constant window area $2a\Delta_\psi \times 2\frac{\Delta_\Psi}{a}\sin\theta{=}4\Delta_\psi\Delta_\Psi\sin\theta$ in the $t-u$ plane. The area depends only on the mother wavelet $\psi(t)$ and the order α (since $\theta = \alpha\pi/2$) and is independent of the parameters a and b. However, for a given order α, the shape of the time-fractional-frequency window varies with the scaling parameter a. Specifically, this window becomes narrower for small values of a and wider for large a. Therefore, the NFRWT provides a flexible time-fractional-frequency window which automatically shrinks when observing high-fractional-frequency phenomena (i.e., small a), and extends when investigating low-fractional-frequency behavior (i.e., large a). From (30), it can be seen that how the time and fractional-frequency resolutions change with the width and height of the time-fractional-frequency window. Figure 2 depicts the difference between time-fractional-frequency windows of the NFRWT and time-frequency windows of the WT.

5 Applications

5.1 Signal denoising

The traditional wavelet denoising methods are often based on the assumption that the energy of the analyzed signal is well concentrated in the frequency domain, since the WT is actually a differently scaled bandpass filter in the frequency domain. In this case, the WT uses a different bandpass filters on the signal filtering. It removes the coefficients of some scales which mainly reflect the noise frequency. Then, the coefficient of every remaining scale is integrated for inverse WT, so that noise can be suppressed well. However, as for signals whose energy is not well concentrated in the frequency domain, the result of this method will not be optimal. It follows from the sampling theory of the FRFT [3] that a nonzero signal whose energy is not well concentrated in the frequency domain may be well focused in a certain fractional domain. For example, chirp signals are this kind of signals. Since the NFRWT is intrinsically a bank of multiscale bandpass filters in the fractional domain, it is suitable for processing such signals. Specifically, the NFRWT can analyze the signal at different fractional-frequency bands with different scales by successive decomposition into coarse approximation and detail information. If the details are small, they might be omitted without substantially affecting the main features of the signal. The idea of thresholding is to set to zero all coefficients that are less than a particular threshold. The modified coefficients are used in an inverse NFRWT to reconstruct the desired signal.

Now, we give an example. The desired signal $s(t)$ is a chirp signal whose chirp rate is -1, and it is interfered by additive white Gaussian noise $n(t)$ with a SNR of 3 dB. The noisy signal $x(t) = s(t) + n(t)$. In the denoising process, we select the db8 wavelet as the mother wavelet and use the universal threshold with hard thresholding rule and three levels of the NFRWT decomposition. To measure the performance of signal denoising, the mean square error (MSE) involving $s(t)$ and its recovered signal $\hat{s}(t)$ is given by

$$\sigma_e^2 = E[|s(t) - \hat{s}(t)|^2]. \tag{31}$$

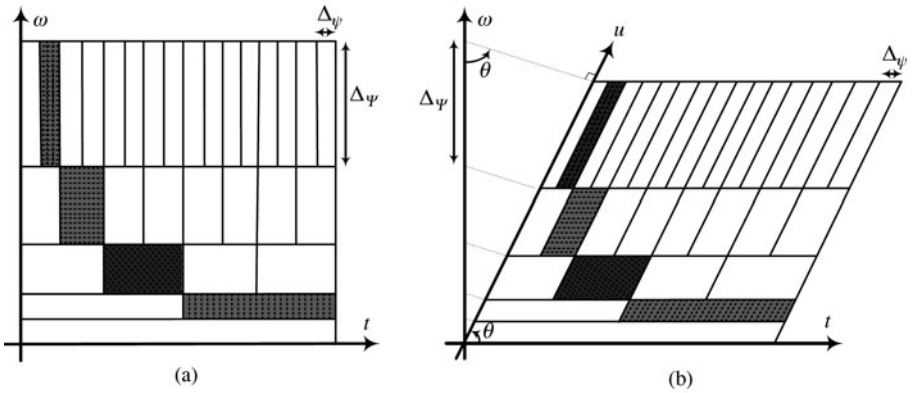

Figure 2 Time-frequency windows of the WT (a) and time-fractional-frequency windows of the NFRWT (b).

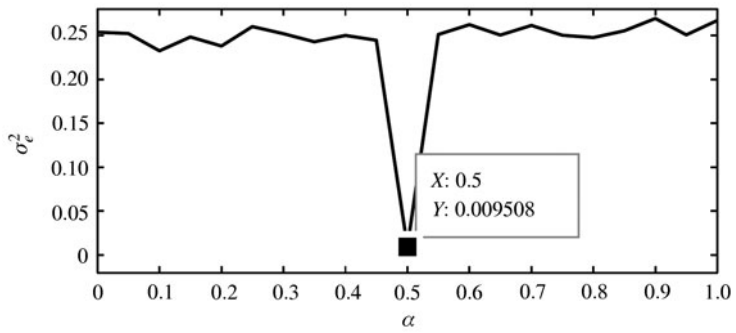

Figure 3 The MSE of signal denoising using the NFRWT with different orders.

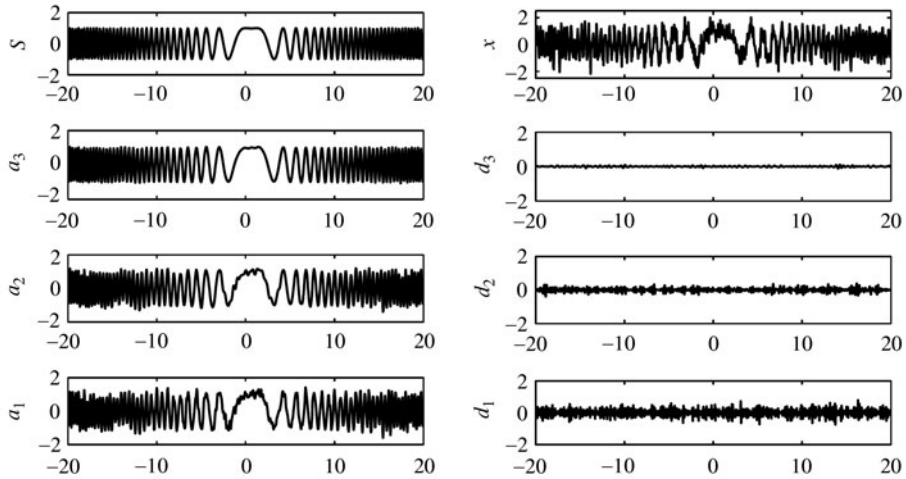

Figure 4 Three levels of the 0.5 th NFRWT decomposition for the interfered signal.

Figure 3 illustrates the MSE of signal denoising using the NFRWT with different orders.

As shown by Figure 3, the NFRWT with $\alpha = 0.5$ has good performance on noise reduction, and the MSE is 9.508×10^{-3}. But for the NFRWT with $\alpha \neq 0.5$, the performance is poor and the MSE is up to about 0.25. Particularly, when $\alpha = 1$, the NFRWT reduces to the WT, and then the MSE is 0.26. According to the relationship between the FRFT and time-frequency distribution [8], this is due to the fact that the energy of $s(t)$ is optimally concentrated only in the 0.5th fractional domain. Figure 4 shows three levels of the 0.5th NFRWT decomposition for the noisy signal.

In Figure 4, time steps and signal amplitude are represented by the horizontal axis and the vertical axis respectively. s and x represent the desired signal and the noisy one, respectively. a_1, a_2, and a_3 are

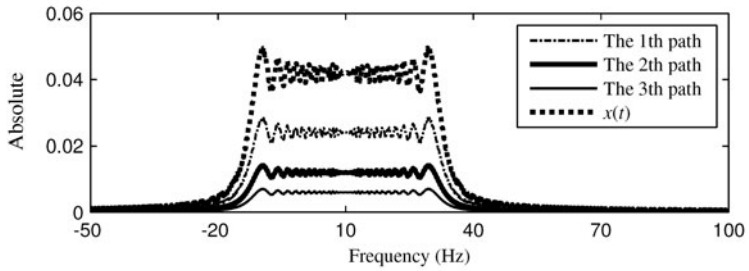

Figure 5 Frequency spectrums of the multipath chirp signal and three path signals.

the coarse approximation of the desired signal at levels 1, 2, and 3. Correspondingly, d_1, d_2, and d_3 are the detail information at levels 1, 2, and 3. Note that the details which reflect noise are small and might be omitted, so that noise can be suppressed well using the above proposed method associated with the NFRWT.

5.2 Multipath chirp signal separation

Since the chirp signal is highly concentrated in the fractional domain and a time delay leads to a fractional-frequency shift, the FRFT is an efficient processing tool for separating multipath chirp signals [14–16]. However, the separation based the FRFT often requires a large number of iterations [14] and is inefficient for practical applications because the FRFT lacks the locality property. The NFRWT is capable of obtaining fractional-domain local properties of a signal and, hence, it can overcome the deficiency of the FRFT based separation. To illustrate this, a multipath chirp signal is modeled as

$$x(t) = \sum_{n=1}^{3} \rho_n \mathrm{e}^{-(\mathrm{j}/2)(t-\tau_n)^2 + \mathrm{j}9.89t}, \tag{32}$$

where ρ_n and τ_n denote the channel gain and the propagation delay of the nth path, respectively. We assume that $\rho_1 = 1$, $\rho_2 = 0.5$, $\rho_3 = 0.25$, $\tau_1 = 0$, $\tau_2 = 7.07$, $\tau_3 = 23.34$. The frequency spectrum of the multipath chirp signal $x(t)$ and that of each path signal are shown in Figure 5.

Note, in Figure 5, each path signal occupies the same frequency band, so they can not be directly separated in the frequency domain efficiently. According to the relationship between the FRFT and time-frequency distribution [8], the multipath chirp signal $x(t)$ is highly concentrated in the 0.5th fractional domain. Moreover, a delay in the time domain results in a shift in the fractional domain and, therefore, the 0.5th NFRWT can separate the signal $x(t)$ efficiently. Figure 6 depicts the results of the separation using the 0.5th NFRWT.

The multipath chirp signal $x(t)$ and its 0.5th FRFT $X_\alpha(u)$ are presented in Figure 6(a)(b), respectively. Here, the absolute of $X_\alpha(u)$ is normalized. Note, in Figure 6(b), $X_\alpha(u)$ contains three fractional frequency components at 7, 12, and 23.5. These components correspond to the 1th, 2th, and 3th path signal, respectively. After separating, the recovered 1th, 2th, and 3th path signals are shown in Figure 6(c)(e)(g). Their corresponding 0.5th FRFT are plotted in Figure 6(d)(f)(h). The MSE of signal separation of the 1th, 2th, and 3th path signals are 4.338×10^{-3}, 5.247×10^{-3}, and 5.103×10^{-3}, respectively. Therefore, the NFRWT can efficiently separate each component of the multipath chirp signal $x(t)$.

6 Conclusions

This paper proposes a novel fractional wavelet transform (NFRWT), which has explicit physical interpretation, i.e., each fractional wavelet component is actually a differently scaled bandpass filter in the fractional domain. Some fundamental results of this transform are presented, including its basic properties, theorems, inverse formula, and admissibility condition. Moreover, the constant-Q property and time-fractional-frequency resolution of the NFRWT are also discussed. The NFRWT is capable of providing the time- and fractional-domain information simultaneously and representing signals in the time-

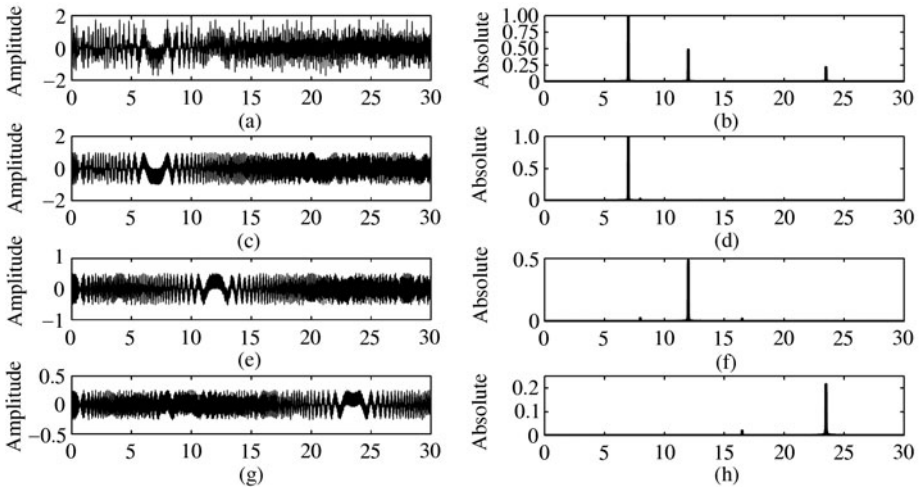

Figure 6 Separating the multipath chirp signal $x(t)$ with 0.5th NFRWT. (a) Multipath chirp signal $x(t)$; (b) FRFT of $x(t)$; (c) the separated 1th path signal; (d) FRFT of the separated 1th path signal; (e) the separated 2th path signal; (f) FRFT of the separated 2th path signal; (g) the separated 3th path signal; (h) FRFT of the separated 3th signal.

fractional-frequency plane. Thus, it can circumvent the limitations of the wavelet transform and the fractional Fourier transform. Unlike those introduced in [4, 7], the proposed transform has low complexity and is easy to implement in practical applications. Finally, the validity of the theoretical results is demonstrated via simulations.

Acknowledgements

This work was supported by National Basic Research Program of China (Grant No. 2007CB310606), and Next-generation Broadband Wireless Mobile Communications Network(Grant No. 2009ZX03004-001).

References

1 Gargour C, Gabrea M, Ramachandran V, et al. A short introduction to wavelets and their applications. IEEE Circ Syst Mag, 2009, 2: 57–68
2 Flandrin P. Time-frequency and chirps. P SPIE, 2001, 4391: 161–175
3 Xia X G. On bandlimited signals with fractional Fourier transform. IEEE Signal Proc Let, 1996, 3: 72–74
4 Mendlovic D, Zalevsky Z, Mas D, et al. Fractional wavelet transform. Appl Optics, 1997, 36: 4801–4806
5 Bhatnagar G, Raman B. Encryption based robust watermarking in fractional wavelet domain. Rec Adv Mult Sig Proc Commun, 2009, 231: 375–416
6 Chen L, Zhao D. Optical image encryption based on fractional wavelet transform. Opt Commun, 2005, 254: 361–367
7 Huang Y, Suter B. The fractional wave packet transform. Multidim Syst Signal Process, 1998, 9: 399–402
8 Tao R, Deng B, Wang Y. Research progress of the fractional Fourier transform in signal processing. Sci China Ser F-Inf Sci, 2006, 49: 1–25
9 Tao R, Li Y L, Wang Y. Short-time fractional Fourier transform and its applications. IEEE Trans Signal Proces, 2010, 58: 2568–2580
10 Wood J C, Barry D T. Linear signal synthesis using the Radon-Wigner transform. IEEE Trans Signal Proces, 1994, 42: 2105–2111
11 Dinç E, Baleanu D. New approaches for simultaneous spectral analysis of a complex mixture using the fractional wavelet transform. Commun Nonlinear Sci Numer Simul, 2010, 15: 812–818
12 Shi J, Chi Y G, Zhang N T. Multichannel sampling and reconstruction of bandlimited signals in fractional domain. IEEE Signal Proc Let, 2010, 17: 909–912
13 Candan C, Kutay M A, Ozaktas H M. The discrete fractional Fourier transform. IEEE Trans Signal Proces, 2000, 48: 1329–1337
14 Tao R, Li X, Li Y, et al. Time-delay estimation of chirp signals in the fractional Fourier transform. IEEE Trans Signal Proces, 2009, 57: 2852–2855
15 Akay O, Erözden E. Employing fractional autocorrelation for fast detection and sweep rate estimation of pulse compression radar waveforms. Signal Process, 2009, 89: 2479–2489
16 Cowell D M J, Freear S. Separation of overlapping linear frequency modulated (LFM) signals using the fractional Fourier transform. IEEE Trans Ultrason Ferr, 2010, 57: 2324–2333